

Superior efficiency for homojunction GaAs solar cell

Ala'eddin A. Saif*, M. Albishri, A. Mindil, M. Qaeed
Physics Department, College of Science, University of Jeddah, Jeddah, Saudi Arabia

This research presents a simulation study to achieve an optimized homojunction GaAs solar cell using SILVACO TCAD. A solar cell with configuration of p⁺-AlGaAs as window, p-GaAs as emitter, n-GaAs as base and n⁺-AlGaInP as BSF layer is proposed. The AlGaInP is selected as BSF layer due to high bandgap as compared to AlGaAs that is usually used in literature. Large scale of variation for doping concentration and thickness for all layers of cell have been simulated. The results show an improvement for solar cell parameters for the optimized cell as compared with the proposed one, where J_{sc} increases from 40.03 mA/cm² to 52.58 mA/cm², V_{oc} slightly increases from 0.94 V to 1 V, P_{max} increases from 30.8 mW/cm² to 46.86 mW/cm², FF increases from 82.19% to 88.54% and η increases from 22.29% to 33.94%. Which confirms the effectiveness of the doping concentration and thickness on solar cell performance.

(Received November 3, 2022; Accepted January 2, 2023)

Keywords: GaAs solar cell, Homojunction, Silvaco, Efficiency, BSF

1. Introduction

Due to the increase demands on energy worldwide and due to the environmental problems caused of using fossil fuels such as coal and oil and the limitation of their lifetime, the world turns to use renewable energy and find new renewable sources of energy which are more environment-friendly [1, 2]. One of the best replacements for fossil fuels is using photovoltaic cells or solar cells, in which the solar energy is converted to electrical energy as illuminated to solar radiation [3]. The simplest structure for solar cells is the one that consists of single junction, then the structure becomes more complex to contain heterojunctions to enable larger amount of solar energy absorption [4].

In the recent few years, many researchers are interested to use GaAs for solar cells fabrication due to its direct band gap of 1.42 eV, which enables it to absorb wide range of solar spectrum energies, large absorption coefficient, high electron mobility, large carrier diffusion length, as well as its ability for doping and fabrication in multiple junctions give GaAs superior advantages to be perfect candidate for high efficiency photovoltaic either in single or multiple junctions solar cells [5-7].

The most challenging issue that degrades the GaAs solar cell performance is the surface recombination, which is usually resolved by introducing Aluminum or Indium doped GaAs layers on top, i.e., window layer, and at bottom, i.e., back surface field (BSF) layer, for the cell [8-9]. A literature survey shows that the conversion efficiency for homojunction GaAs varies between 13.75% to 29.75% depending on the cell configuration [3, 6-7, 10-12]. Based on literature, it is also found that most of researchers use AlGaAs as window and BSF layers in single junction GaAs solar cell, however, few studies present AlGaInP as window but not as BSF layer [3, 6-7, 10-12]. Therefore, in this work, AlGaInP has been introduced as BSF layer for single junction GaAs cell depending on its high energy bandgap as compared to AlGaAs. Then, a comprehensive investigation for the effect of a large-scale variation of doping concentration and thickness of all solar cell layers, which is configured as p⁺-AlGaAs for window, p-GaAs for emitter, n-GaAs for base and n⁺-AlGaInP for BSF, have been carried out with the aid of SILVACO TCAD to achieve the optimum performance for the proposed cell.

* Corresponding author: aasaif@uj.edu.sa
<https://doi.org/10.15251/JOR.2023.191.1>

2. Structure and modeling

Numerical simulation approach for solar cells is trusted technique and is widely used since it allows to study many parameters at different conditions in shorter time with less cost compared to fabrication method that required high advanced facilities with hefty cost. SILVACO TCAD has been used by many researchers to simulate solar cell [4, 7, 13-15]. It works based on mathematical models that consist of fundamental equations such as Poisson's equation, continuity equation, and transport equations.

The simulation starts with developing the solar cell structure using ATLAS simulator from silvaco international by setting the mesh and specifying the regions geometry as illustrated in Figure 1(a). Then the doping profile and material parameters, which are tabulated in Table 1, for the regions are defined. This step is followed by specifying the physical model that ATLAS will use during simulation. The models used in simulation are Shockley-Read-Hall (SRH), Fermi distribution (FERMI), concentration dependent mobility (conmob), Optical recombination (optr), AUGER recombination (AUGER) and bandgap narrowing (bgn). Once the cell is developed in ATLAS, it is illuminated by a light source defining the beam power and its respective wavelength to get the photoresponse for the cell, the irradiation spectrum for AM1.5G that is used in this study is illustrated in Figure 1(b). In order to obtain the output of electrical characteristics for the cell, statements to extract the short circuit current density (J_{sc}), open circuit voltage (V_{oc}), maximum power (P_{max}), fill factor (FF) and conversion efficiency (η) are set on ATLAS simulator.

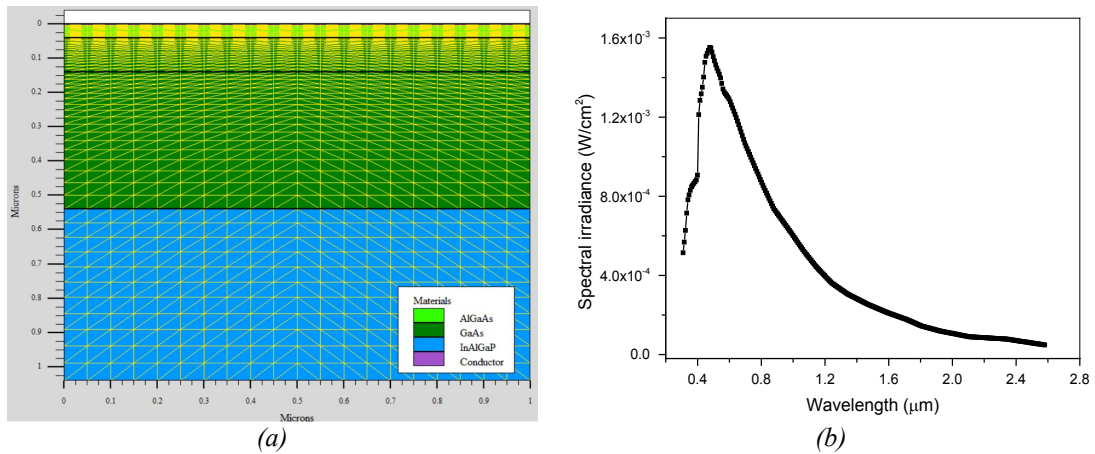


Fig. 1. (a) Meshing and regions for proposed solar cell and (b) AM1.5 spectrum used to illuminate the solar cell.

Table 1. Material parameters used in solar cell simulation [15].

Material	$Al_{0.8}Ga_{0.2}As$	GaAs	$(Al_{0.7}Ga_{0.3})_{0.5}In_{0.5}P$
Energy bandgap (eV)	2.09	1.42	2.4
Permittivity	11.7	13.2	11.7
Affinity (eV)	3.53	4.07	4.2
MUN (cm^2/Vs)	212.2	8800	2150
MUP (cm^2/Vs)	67.6	400	141
NC300 (cm^{-3})	$1.58e^{19}$	$4.35e^{17}$	$1.2e^{20}$
NV300 (cm^{-3})	$1.5e^{19}$	$1.29e^{19}$	$1.28e^{19}$
TAUN (s)	$1e^{-9}$	$1e^{-9}$	$1e^{-9}$
TAUP (s)	$2e^{-8}$	$2e^{-8}$	$1e^{-9}$

In this work, the proposed single junction solar cell is configured as: p^+ - $\text{Al}_{0.8}\text{Ga}_{0.2}\text{As}$ is used to represent the window layer, its energy bandgap of 2.09 eV is higher than the bandgap for GaAs of 1.42 to enable absorbing light of short wavelength, p -GaAs represents the emitter layer for absorber material, n -GaAs represents the base layer for absorber material and n^+ - $(\text{Al}_{0.7}\text{Ga}_{0.3})_{0.5}\text{In}_{0.5}\text{P}$ with bandgap of 2.4 which is larger than bandgap for GaAs also to represent the back surface field (BSF) layer. The energy bands diagram for the proposed solar cell is illustrated in Figure 2(a). Basically, the proposed thickness for these layers is 0.004 μm , 0.01 μm , 0.4 μm and 0.5 μm , respectively. While the doping concentration is set as $3 \times 10^{18} \text{ cm}^{-3}$, $1 \times 10^{18} \text{ cm}^{-3}$, $1 \times 10^{16} \text{ cm}^{-3}$, $1 \times 10^{19} \text{ cm}^{-3}$, respectively. The doping scale and thickness for layers are depicted in Figure 2(b). The impact of layers doping concentration and thickness on the electrical parameters of the basic cell has been investigated in order to achieve the optimum conversion efficiency for the proposed cell.

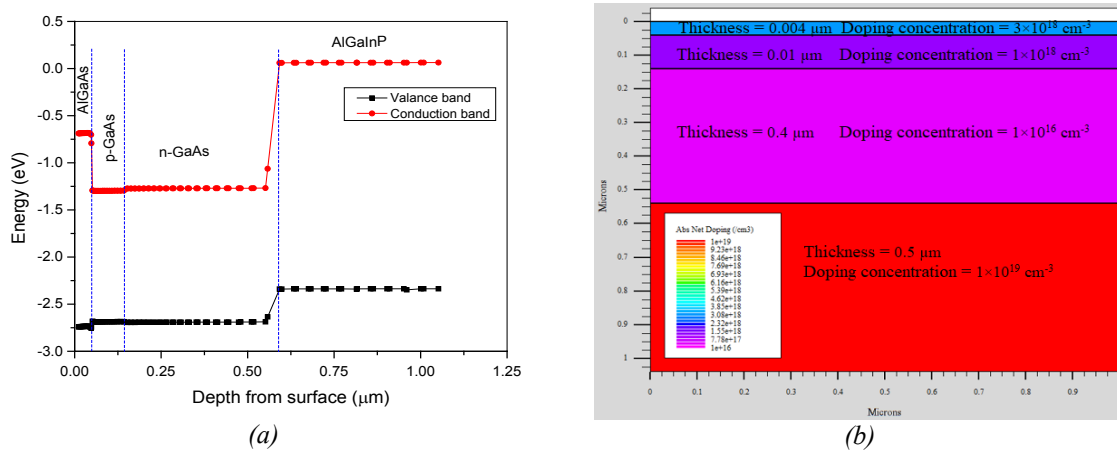


Fig. 2. (a) Energy bands diagram and (b) Doping level and thickness for layers for the proposed solar cell.

3. Results and Discussion

3.1. Basic Solar Cell

After simulating the basic solar cell described earlier using the parameters in Table 1 in addition to the proposed layer thickness and doping concentration, the current-voltage (I-V) curve is extracted and plotted as shown in Figure 3. From I-V characteristics the short circuit current density (J_{sc}), open circuit voltage (V_{oc}), maximum power (P_{max}), fill factor (FF) and solar efficiency (η) can be determined. The obtained value for J_{sc} , V_{oc} , P_{max} , FF and η for basic cell is 40.03 mA/cm^2 , 0.94 V, 30.8 mW/cm^2 , 82.19% and 22.29%, respectively.

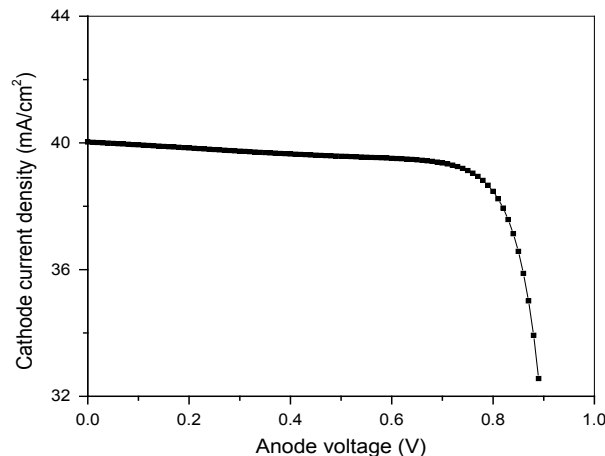


Fig. 3. I-V characteristics for basic solar cell.

3.2. Impact of AlGaAs Window Doping and Thickness

Window layer on top of absorber material in solar cell considers an important layer to minimize the surface recombination in absorber layer. In this work, p-Al_{0.8}Ga_{0.2}As with a bandgap of 2.09 eV is chosen. The higher value of bandgap for Al_{0.8}Ga_{0.2}As as compared to GaAs, make it transparent for the photons of energy less than 2.1 eV, thus more photons would be allowed to be absorbed by cell. The effect of window acceptor doping concentration on cell performance is investigated by changing the concentration over seven orders of magnitude from $3 \times 10^{15} \text{ cm}^{-3}$ to $3 \times 10^{21} \text{ cm}^{-3}$. The doping concentration for emitter, base and BSF layers is fixed at $1 \times 10^{18} \text{ cm}^{-3}$, $1 \times 10^{16} \text{ cm}^{-3}$ and $1 \times 10^{19} \text{ cm}^{-3}$, respectively. The variation of J_{sc} , V_{oc} , P_{max} and η with acceptor doping concentration is shown in Figure 4. It is noticed that the effect of acceptor doping level for window layer has weak impact on the value of all cell parameters. For instant, the efficiency of the solar cell increases from 22.11% to 22.44% as the doping concentration increases from $3 \times 10^{15} \text{ cm}^{-3}$ to $3 \times 10^{17} \text{ cm}^{-3}$, then decreases to 22.24% as the doping concentration increases to $3 \times 10^{19} \text{ cm}^{-3}$, and then remains constant until $3 \times 10^{21} \text{ cm}^{-3}$ doping level. This decrement in efficiency at certain doping level could be due to the increase of charge density, thus as window layer is illuminated, the optical generation increases, which in turn increases the recombination rate in cell layers, as a result reduce the performance of cell [20]. Similar variation trend for J_{sc} , V_{oc} , P_{max} is observed. Interestingly, all these parameters show maximum value at $3 \times 10^{17} \text{ cm}^{-3}$ doping level. Therefore, this doping concentration is considered the optimum doping for window layer.

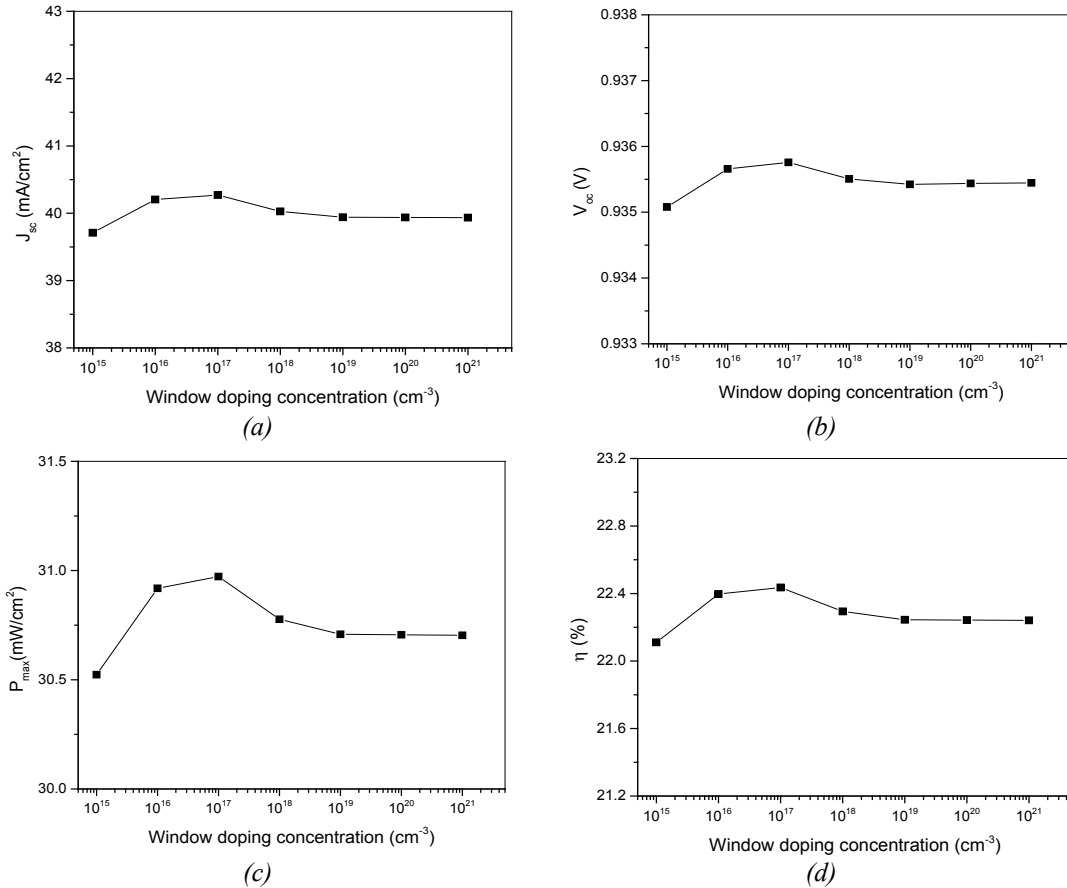


Fig. 4. Effect of p-AlGaAs window doping concentration variation on GaAs solar cell performance (a) J_{sc} , (b) V_{oc} , (c) P_{max} and (d) η .

In order to study the effect of window thickness on the cell performance, the J_{sc} , V_{oc} , P_{max} and η are plotted with respect to the thickness as shown in Figure 5. The window thickness increases from 0.005 μm to 0.05 μm with a step of 0.005 μm while the thickness of emitter, base

and BSF layers is fixed at 0.1 μm , 0.4 μm and 0.5 μm , respectively. All parameters show almost linear relatively weak decrement variation with window thickness. For example, the P_{max} reduces from 31.91 mW/cm^2 to 30.54 mW/cm^2 while conversion efficiency reduces from 23.12% to 22.12% as the window thickness increases from 0.005 to 0.05 μm . This indicates that lower window thickness gives better cell performance, which is attributed to maximize the amount of photon transmitted into the absorber material [9]. From parameter graphs can be found that 0.005 is the optimum thickness for the window.

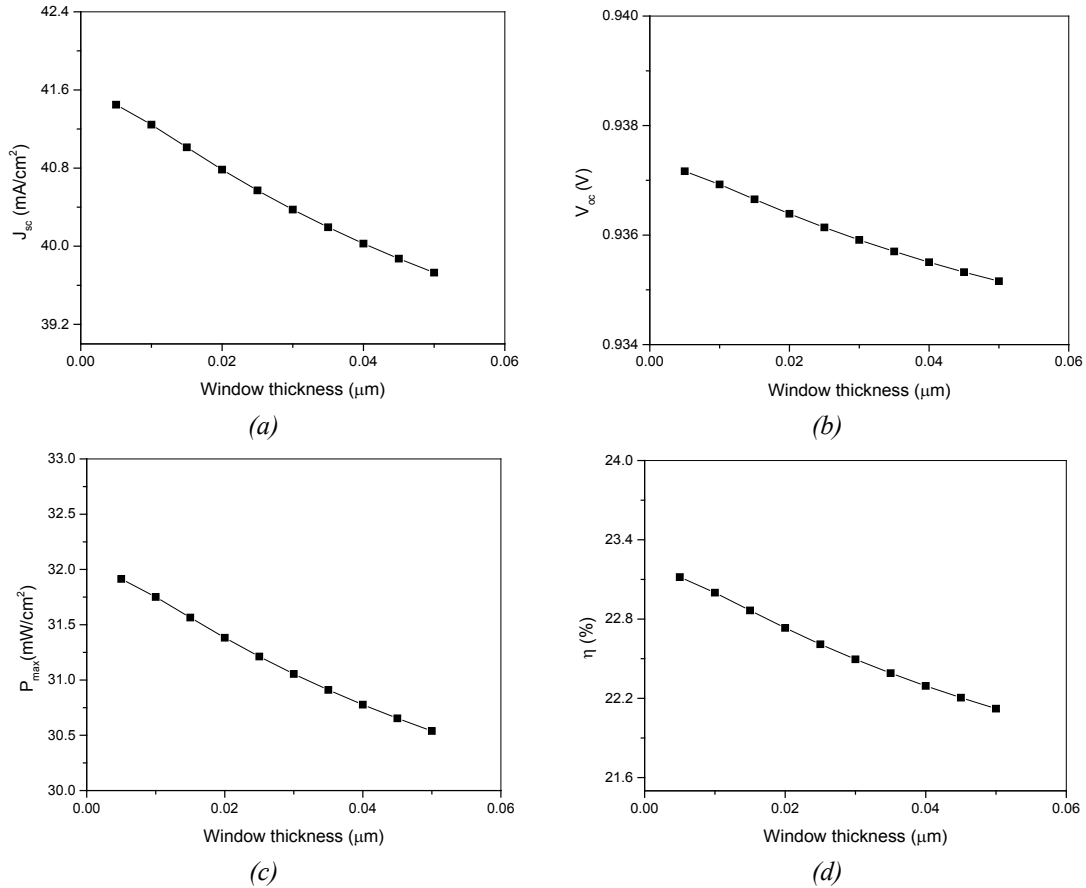


Fig. 5. Effect of p-AlGaAs window thickness variation on GaAs solar cell performance (a) J_{sc} , (b) V_{oc} , (c) P_{max} and (d) η .

3.3. Impact of GaAs Emitter Doping and Thickness

Controlling the doping concentration of emitter layer is essential to optimize the efficiency of solar cell, since the emitter doping determine the amount of charge carrier generated and the recombination rate within this layer. For the current cell, p-GaAs is considered to represent the emitter layer, where the doping concentration is changed over nine orders of magnitude from $6 \times 10^{17} \text{ cm}^{-3}$ to $5 \times 10^{18} \text{ cm}^{-3}$ to investigate its effect on cell performance. The doping concentration for window, base and BSF layers is fixed at $3 \times 10^{18} \text{ cm}^{-3}$, $1 \times 10^{16} \text{ cm}^{-3}$ and $1 \times 10^{19} \text{ cm}^{-3}$, respectively. Figure 6 illustrates the effect of acceptor doping level for GaAs on J_{sc} , V_{oc} , P_{max} and η for the cell. It is noted that increasing the doping concentration for emitter does not much effect on all parameters. For instant, the J_{sc} weakly increases from 40.018 mA/cm^2 to 40.029 mA/cm^2 as the doping level increases from $6 \times 10^{17} \text{ cm}^{-3}$ to $1 \times 10^{18} \text{ cm}^{-3}$ then decreases to 40.017 mA/cm^2 at $5 \times 10^{18} \text{ cm}^{-3}$. Generally, increasing the acceptor doping more than some limitation reduces the minority carrier lifetime which in turn reduces the short circuit current [16]. V_{oc} is also weakly increased along doping variation range. η shows almost constant value of 22.294% until doping level of

$1 \times 10^{18} \text{ cm}^{-3}$ then decreases to 22.277% at $5 \times 10^{18} \text{ cm}^{-3}$. Based on all graphs, the optimum doping concentration for emitter is found to be $1 \times 10^{18} \text{ cm}^{-3}$.

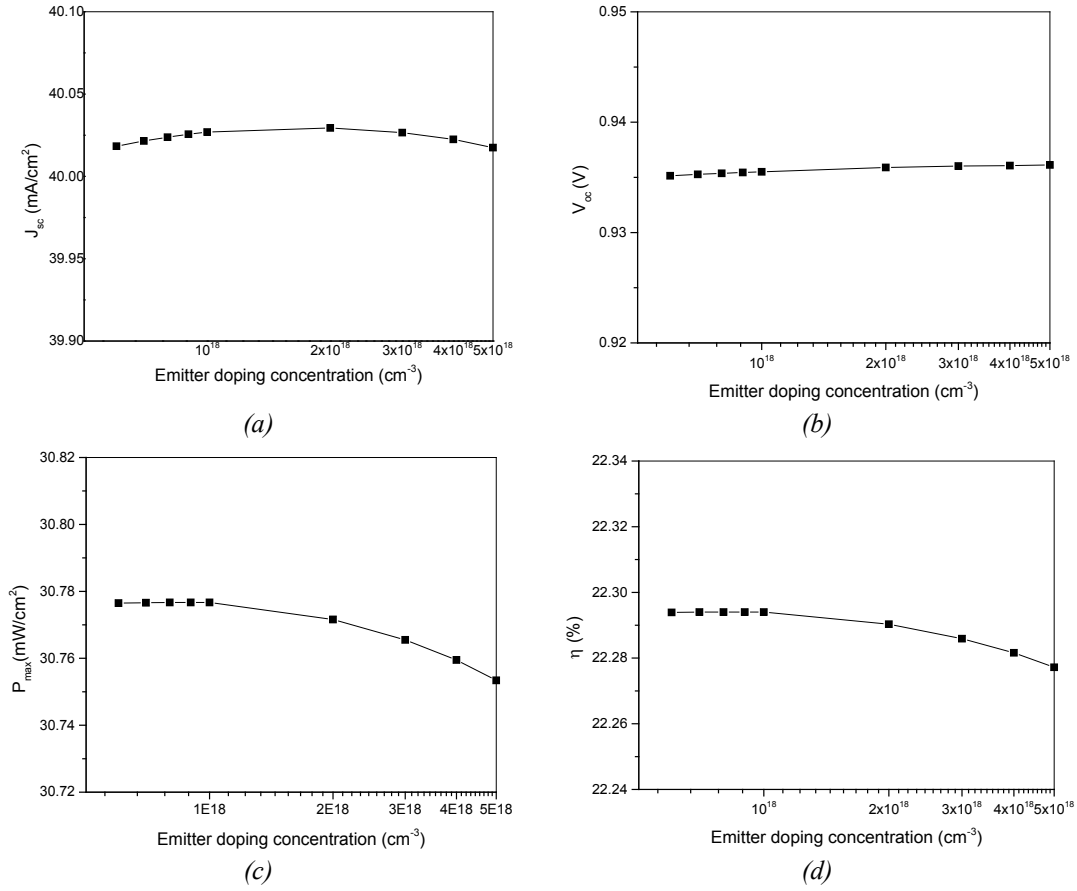


Fig. 6. Effect of p-GaAs emitter doping concentration variation on GaAs solar cell performance (a) J_{sc} , (b) V_{oc} , (c) P_{max} and (d) η .

The variation of J_{sc} , V_{oc} , P_{max} and η as a function of emitter thickness for the cell is shown in Figure 7. The emitter thickness increases from 0.1 μm to 0.4 μm with a step of 0.02 μm while the thickness of window, base and BSF layers is fixed at 0.04 μm , 0.4 μm and 0.5 μm , respectively. It can be noticed that the cell parameters notably change with emitter thickness. Whereas J_{sc} shows continues increasing with emitter thickness until 0.4 μm while V_{oc} shows decrement trend with emitter thickness until 0.36 μm then slightly increases at thicker emitter. Increasing the emitter thickness enhances the probability of photon interaction and generates more electron-hole pairs within the emitter region, which in turn enhances the short circuit current, consequently, decreases the open circuit voltage [17]. The maximum power increases from 30.78 mW/cm² to 32.15 mW/cm² as the emitter thickness increases from 0.1 μm to 0.36 μm then comparably decreases at thicker layer. Similar trend for conversion efficiency as P_{max} is observed, where the optimum conversion efficiency of 23.29% is obtained at 0.36 μm thickness. The efficiency increment can be explained based on electron-hole carrier generation, however, as the emitter exceeds 0.36 μm thick, the carriers move longer distances as compared to their diffusion length, thus their probability to be recombined is higher than to be collected on contact [18], which explains the reduction in efficiency at thickness more than 0.36 μm . Based on cell parameter values, the optimal emitter thickness is 0.36 μm .

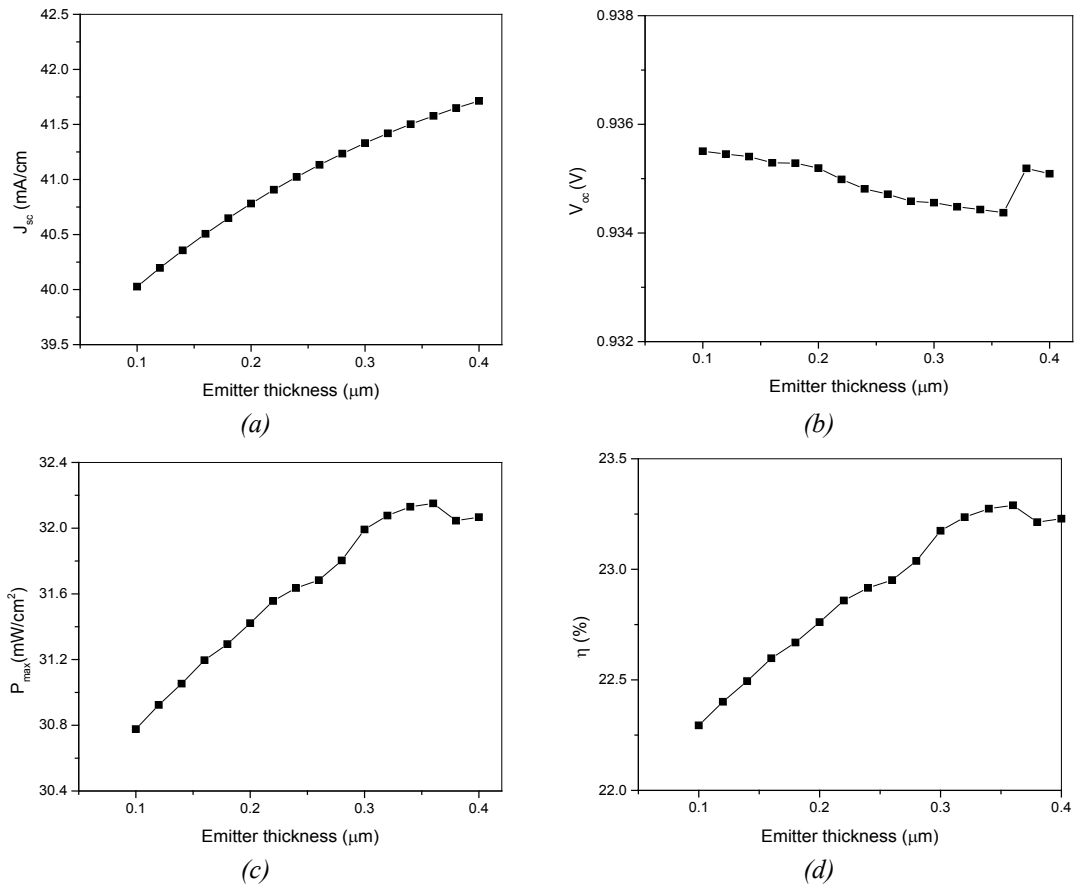


Fig. 7. Effect of p-GaAs emitter thickness variation on GaAs solar cell performance (a) J_{sc} , (b) V_{oc} , (c) P_{max} and (d) η .

3.4. Impact of GaAs Base Doping and Thickness

Doping concentration for base layer needs to be engineered carefully since it is directly influenced the efficiency of the solar cell. When the base doping is low resultant in not enough electron-hole pairs generation. Whereas the doping is highly concentrated leading to increase the recombination rate for the carriers [19]. Thus, donor doping concentration for n-GaAs base layer is changed over eighteen orders of magnitude from $1 \times 10^{15} \text{ cm}^{-3}$ to $9 \times 10^{16} \text{ cm}^{-3}$ to investigate its effect on cell parameters, and the results are plotted in Figure 8. The doping concentration for window, emitter and BSF layers is fixed at $3 \times 10^{18} \text{ cm}^{-3}$, $1 \times 10^{18} \text{ cm}^{-3}$ and $1 \times 10^{19} \text{ cm}^{-3}$, respectively. From the figure it is noticed that increasing the doping concentration for base has significant effect on all parameters. For example, J_{sc} weakly decreases from 40.4 mA/cm² to 40.03 mA/cm² as the doping increases from $1 \times 10^{15} \text{ cm}^{-3}$ to $1 \times 10^{16} \text{ cm}^{-3}$, then it decreases dramatically to 34.06 mA/cm² at $9 \times 10^{16} \text{ cm}^{-3}$. V_{oc} increases from 0.9 V at doping concentration of $1 \times 10^{15} \text{ cm}^{-3}$ to 1 V at concentration of $4 \times 10^{16} \text{ cm}^{-3}$ then attain to almost constant value until $9 \times 10^{16} \text{ cm}^{-3}$. P_{max} shows increase from 29.4 mW/cm² at doping concentration of $1 \times 10^{15} \text{ cm}^{-3}$ to 30.79 mW/cm² at concentration of $9 \times 10^{15} \text{ cm}^{-3}$ then decreases to 28.3 mW/cm² at concentration of $9 \times 10^{16} \text{ cm}^{-3}$. Similar behavior for efficiency as P_{max} is observed, where the efficiency increases from 21.29% at doping concentration of $1 \times 10^{15} \text{ cm}^{-3}$ to 22.30% at concentration of $9 \times 10^{15} \text{ cm}^{-3}$ then decreases to 20.50% at concentration of $9 \times 10^{16} \text{ cm}^{-3}$. Increasing the doping concentration in base layer causes to decrease the carrier mobility thus reduces the resistivity for the base, as a result, increases the open circuit voltage, consequently, decreases the short circuit current [12]. At the same time high doping level causes higher recombination rate, which degrades the conversion efficiency [19]. From the results, it can be concluded that $9 \times 10^{15} \text{ cm}^{-3}$ is the optimum doping concentration for base in the proposed cell.

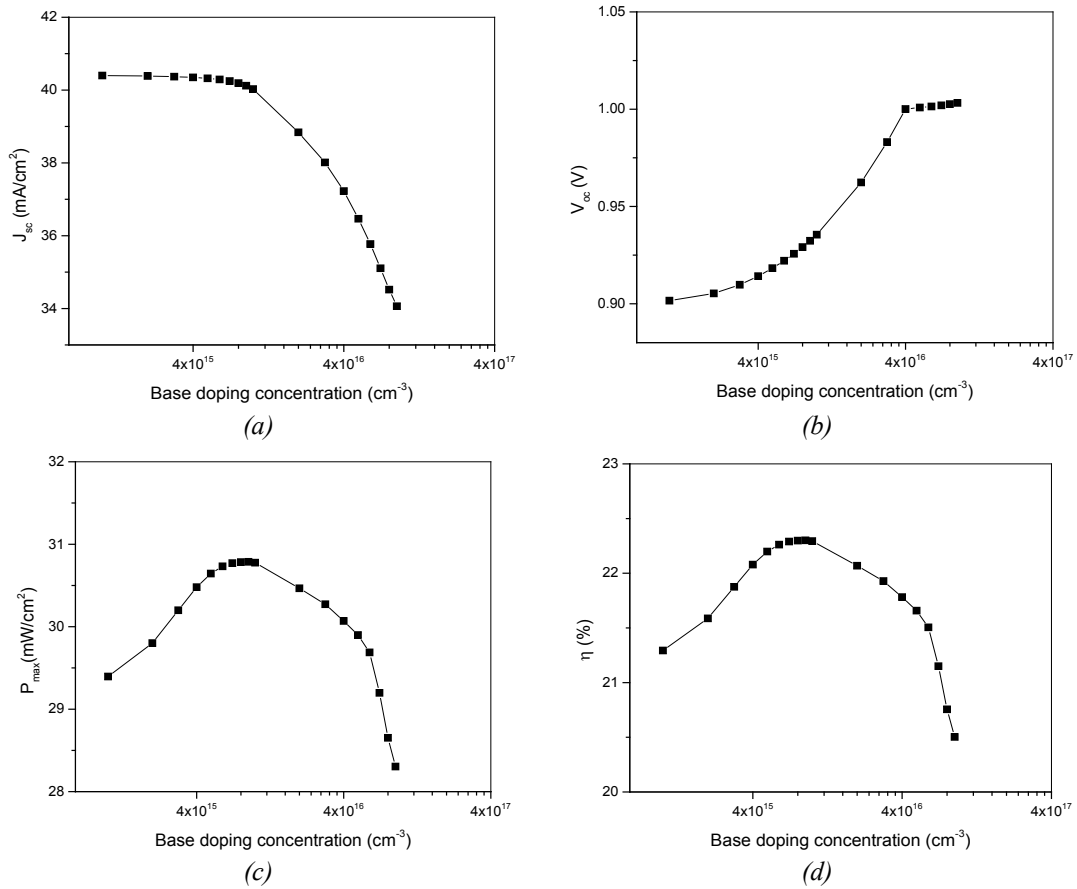


Fig. 8. Effect of n-GaAs base doping concentration variation on GaAs solar cell performance (a) J_{sc} , (b) V_{oc} , (c) P_{max} and (d) η .

The dependent of J_{sc} , V_{oc} , P_{max} and η on base thickness for the cell is shown in Figure 9. The base thickness increases from 0.4 μm to 1.9 μm with a step of 0.1 μm while the thickness of window, emitter and BSF layers is fixed at 0.04 μm , 0.1 μm and 0.5 μm , respectively. It can be noticed that the cell parameters remarkably change with base thickness. Whereas J_{sc} exponentially increases from 40.03 mA/cm² to 43.1 along thickness variation range. While V_{oc} almost linearly decreases from 0.936 V to 0.924 V along thickness variation. The maximum power exponentially increases from 30.78 mW/cm² to 33.43 mW/cm² as the base thickness increases until 1.7 μm then slightly decreases to 33.41 mW/cm² for thicker base. Similar trend for conversion efficiency as P_{max} is observed where it is exponentially increased from 22.29% to 24.22% as the base thickness increases until 1.7 μm then slightly decreases to 24.2% for higher thickness. The increase in short circuit current density and conversion efficiency with base thickness is attributed to the increase of absorption probability for the photons of longer wavelength, which in turn increases the photo-generated carriers [3]. Further increase in base thickness weakly decreases the efficiency, for instant as the thickness increases to 2.5 μm the conversion efficiency reaches to 24%. Based on cell parameter values, the optimal base thickness that gives maximum power and efficiency is 1.7 μm .

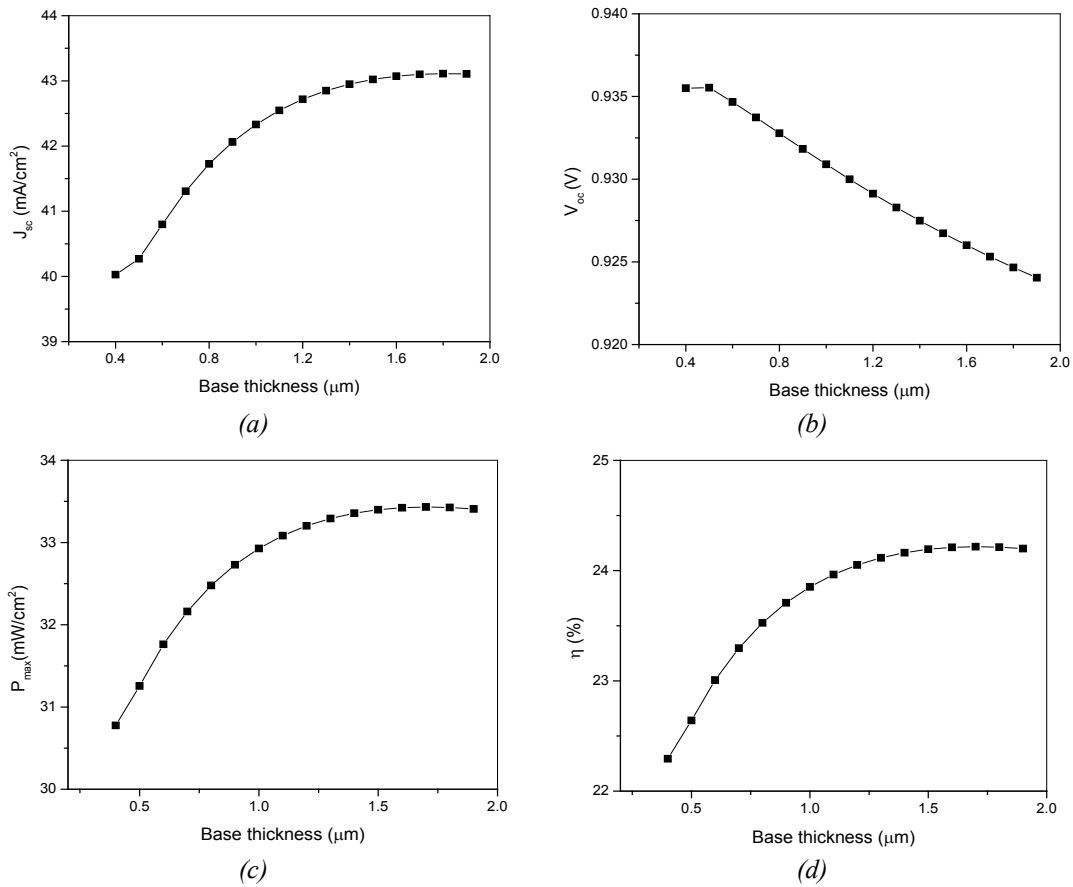


Fig. 9. Effect of n-GaAs base thickness variation on GaAs solar cell performance (a) J_{sc} , (b) V_{oc} , (c) P_{max} and (d) η .

3.5. Impact of AlGaInP BSF Doping and Thickness

BSF layer at the bottom of absorber material in solar cell considers an important layer to minimize the surface recombination and carrier annihilation at the backside of the cell. For this matter n-(Al_{0.7}Ga_{0.3})_{0.5}In_{0.5}P with a bandgap of 2.4 eV, which is relatively higher than GaAs, is used. The doping of BSF layer play significant role on solar cell performance. Therefore, the effect of donor doping level for n-(Al_{0.7}Ga_{0.3})_{0.5}In_{0.5}P is investigated by changing the doping concentration over eleven orders of magnitude from 1×10^{13} cm⁻³ to 1×10^{23} cm⁻³. The doping level for window, emitter and base layers is fixed at 1×10^{17} cm⁻³, 1×10^{18} cm⁻³ and 1×10^{16} cm⁻³, respectively. The variation of J_{sc} , V_{oc} , P_{max} and η with doner doping concentration for BSF layer is shown in Figure 10. It is noticed that the doner doping level for BSF remarkably enhances the cell efficiency. Where J_{sc} , P_{max} and η illustrate strong increment at low doping from 1×10^{13} cm⁻³ to 1×10^{17} cm⁻³ then slightly increase at higher doping level up to 1×10^{23} cm⁻³. The J_{sc} increases from 32.4 mA/cm² to 40.4 mA/cm², P_{max} increases from 22.77 mW/cm² to 30.84 mW/cm² and the efficiency increases from 16.5% to 22.87% along the doping level variation. Highly dopped BSF layer tends to create high electric field at the backside of the cell, this field repels the separated carriers toward the space charge region, which decreases the recombination rate for carriers, consequently, increases the output current and cell efficiency [6]. One of drawback for BSF layer is by creating backside field, thus, the open circuit voltage increases as shown in figure 10(b) [6], where V_{oc} shows slow increment at low and high doping concentration, however, it shows dramatical increment in the middle doping level range. Where, V_{oc} changes from 0.91 V to 0.945 V along doping variation, which is still in less than 1 V. Interestingly, further increment for doping concentration higher than 1×10^{23} cm⁻³ is not possible, which could be due structure damage for the

solar cell, therefore, $1 \times 10^{23} \text{ cm}^{-3}$ is considered as the optimum doping level for BSF layer in the proposed cell.

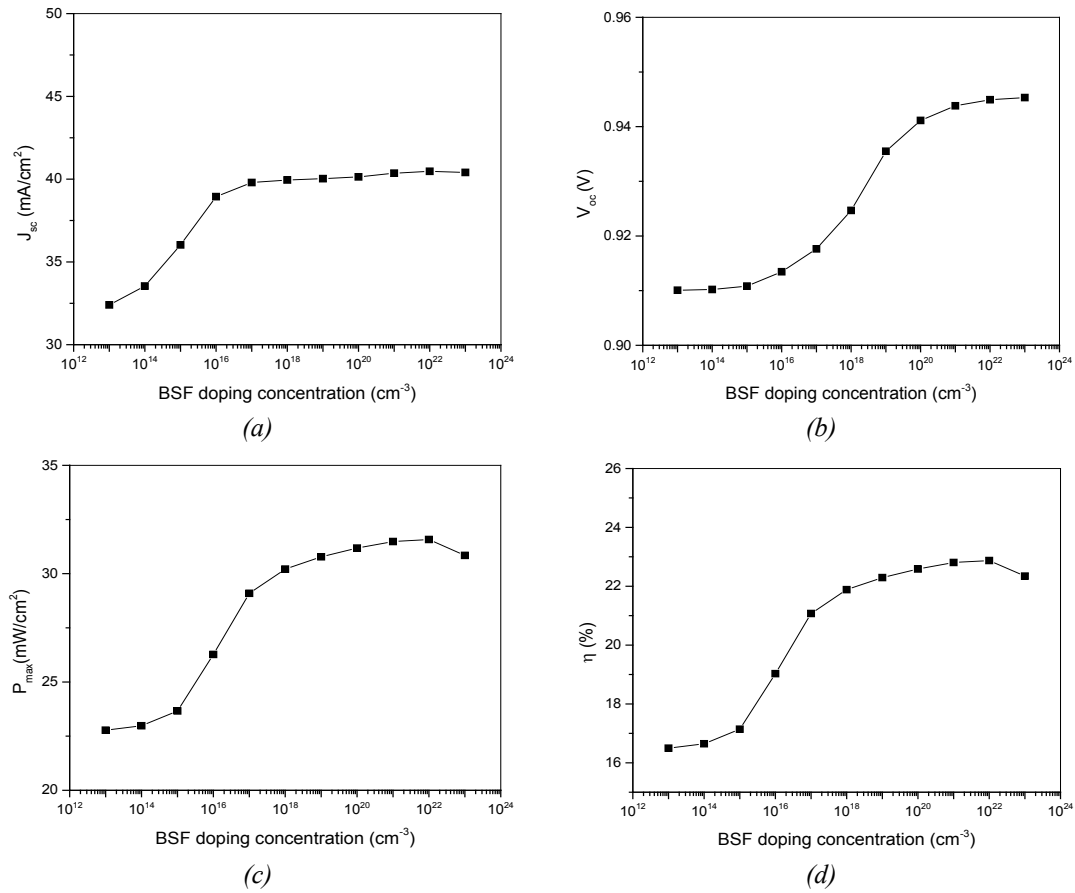


Fig. 10. Effect of $n\text{-}(Al_{0.7}Ga_{0.3})_{0.5}In_{0.5}P$ BSF doping concentration variation on GaAs solar cell performance (a) J_{sc} , (b) V_{oc} , (c) P_{max} and (d) η .

The impact of BSF layer thickness on the cell performance is studied by varying its thickness from $0.1 \mu\text{m}$ to $2 \mu\text{m}$ with $0.1 \mu\text{m}$ step, while the thickness of window, emitter and base layers is fixed at $0.04 \mu\text{m}$, $0.1 \mu\text{m}$ and $0.4 \mu\text{m}$, respectively. The J_{sc} , V_{oc} , P_{max} and η are plotted as a function of BSF thickness as shown in Figure 11. It can be noticed that all parameters show an exponential increase, that starts with strong increment until BSF thickness of $1.2 \mu\text{m}$ then continue with weak increase up to BSF thickness of $2 \mu\text{m}$. For example, J_{sc} increases from 31.13 mA/cm^2 to 49.57 mA/cm^2 , P_{max} increases from 24.05 mW/cm^2 to 38.3 and the efficiency increases from 17.42% to 27.74% as the BSF layer thickness increases from 0.1 to $2 \mu\text{m}$. This indicates that the BSF thickness has significant impact to improve cell efficiency and give better performance, which is attributed to maximize and confined the photogenerated carriers within the pn absorber junction [14]. It is important to mention here that the open circuit voltage increases with increasing the BSF layer thickness as shown Figure 11(b), which could be because of more carriers are accumulated at the edges of solar cell. It is interesting to mention here that further increase in the BSF thickness slightly improves the cell efficiency, however, due to weak effect of increase the BSF thickness beyond $2 \mu\text{m}$, the simulation is stopped at this value, which it is considered the optimum thickness for the BSF layer.

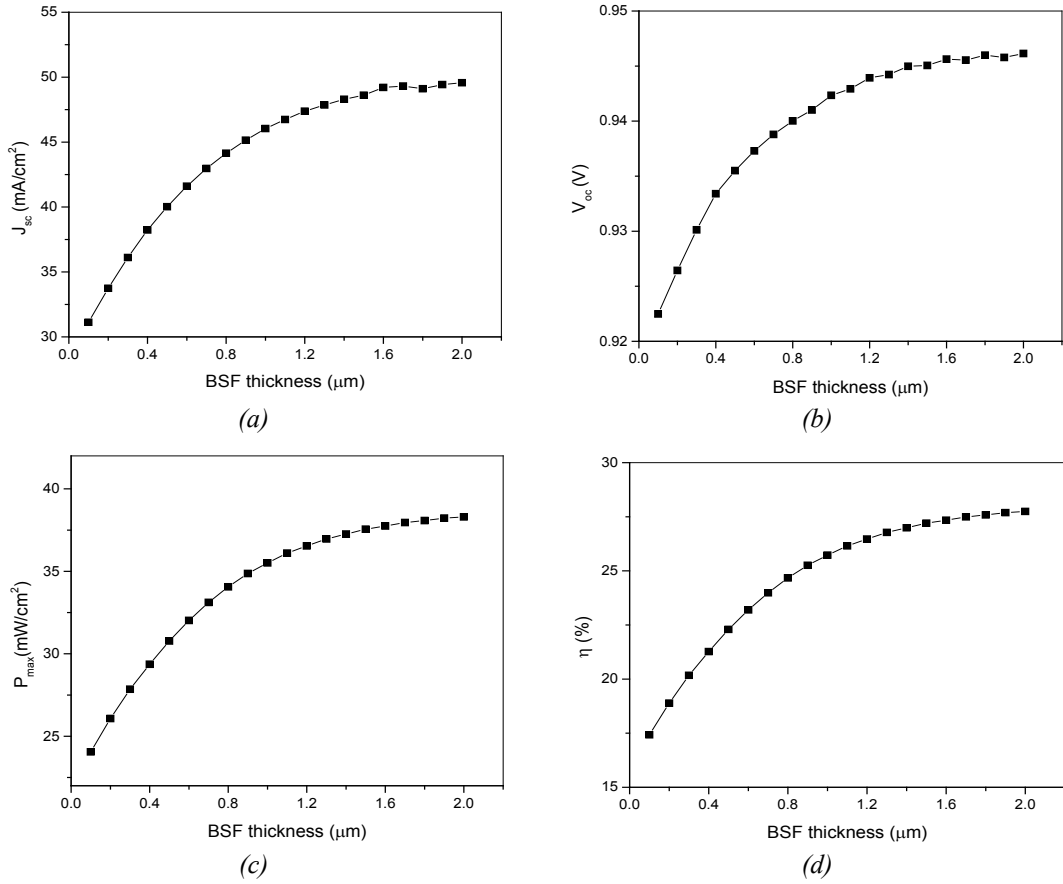


Fig. 11. Effect of n -(Al_{0.7}Ga_{0.3})_{0.5}In_{0.5}P BSF thickness variation on GaAs solar cell performance (a) J_{sc} , (b) V_{oc} , (c) P_{max} and (d) η .

3.6. Optimize solar cell

Based on the results of efficiency variation at different layer thickness and doping concentration for the basic solar cell configuration, which consists of p-AlGaAs as a window, p-GaAs as an emitter, n-GaAs as a base and n-AlGaInP as a BSF layer. It is found that the optimum thickness for the window, emitter, base and BSF layers is 0.005 μm , 0.36 μm , 1.7 μm and 2 μm , respectively. In addition, the optimum doping level for these layers is $3 \times 10^{18} \text{ cm}^{-3}$, $1 \times 10^{18} \text{ cm}^{-3}$, $3 \times 10^{17} \text{ cm}^{-3}$, $1 \times 10^{22} \text{ cm}^{-3}$, respectively. These values of thickness and doping are simulated for an optimize solar cell and its IV characteristics is plotted as shown in figure 12(a). From the figure it is found that the short circuit current density is 52.58 mA/cm², the open circuit voltage is 1 V, the maximum power is 46.86 mW/cm², the fill factor is calculated to be 88.54% and the efficiency is 33.94%. A comparison between the optimized and the basic solar cells are summarized in Table 2. It can be noticed the improvement in all electrical parameters for the optimized solar cell as compared to the basic cell, this confirms controlling the thickness and doping concentration for solar cell regions has significant impact on improving the cell performance. In order to explain the high efficiency of the optimized cell in this work, a cutline view for the photogeneration rate along the solar cell is plotted as shown in figure 12(b). It is clearly that the photogeneration rate along the cell is relatively high including inside the BSF layer. Whereas the photogeneration rate shows highest rate at the surface of the emitter region and reduces exponentially along the base region, then it suddenly increases to relatively high rate inside the BSF layer and slightly decreases along it. The increase in the photogeneration rate within the AlGaInP indicates that this layer share with the total photocurrent of the cell, consequently, increases its efficiency.

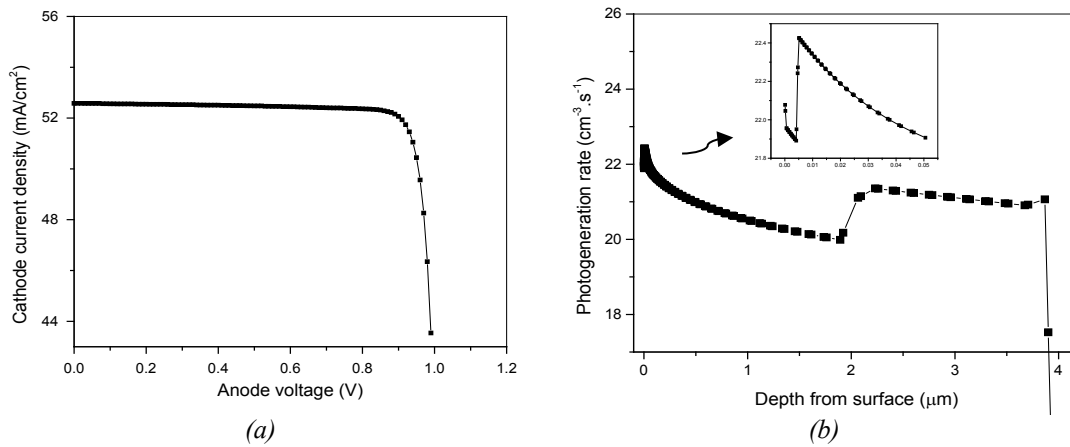


Fig. 12. (a) I - V characteristics and (b) cutline view for photogeneration rate for optimized solar cell.

Table 2. Comparison between basic solar cell and optimized solar cell.

Parameter	Basic solar cell	Optimized solar cell
J_{sc} (mA/cm^2)	40.03	52.58
V_{oc} (V)	0.94	1
P_{max} (mW/cm^2)	30.8	46.86
FF (%)	82.19	88.54
η (%)	22.29	33.94

As comparison for our optimized single junction GaAs solar cell results with others introduced by researchers in previous studies, number of reports are listed in Table 3. It can be obviously noticed that the highly efficient performance for our cell. We believe that the difference in our cell performance could be related to large scale for parameters variation, specifically the thickness and doping concentration, during simulation. Besides, using $(\text{Al}_{0.7}\text{Ga}_{0.3})_{0.5}\text{In}_{0.5}\text{P}$ as BSF layer which has higher energy bandgap of 2.4 eV as compared to $\text{Al}_{0.8}\text{Ga}_{0.2}\text{As}$ with bandgap of 2.09 eV, which is usually used by most of researcher as BSF, gives more advantage to confine more photogenerated carriers within pn absorber region. As well as it works on maintaining the photogeneration rate for the carriers along the cell as shown in figure 12(b).

Table 3. Comparison between our optimized single junction GaAs solar cell and other cells from literature.

Researcher	Efficiency
César Palacios et al. [3]	< 25%
Hemmani et al. [6]	26.58%
Kamal Attari et al. [7]	29.75%
Imran, et al. [10]	13.75%
Mohammed Azza at al. [11]	21.05%
M. Abderrezek et al. [12]	25.8%

4. Conclusion

A single junction GaAs solar cell, with the configuration of p-AlGaAs as window, p-GaAs as emitter, n-GaAs as base and n-AlGaInP as BSF layer, is simulated to achieve the optimal conversion efficiency using SILVACO TCAD simulator. The basic cell starts with layers doping concentration of $3 \times 10^{18} \text{ cm}^{-3}$, $1 \times 10^{18} \text{ cm}^{-3}$, $1 \times 10^{16} \text{ cm}^{-3}$, $1 \times 10^{19} \text{ cm}^{-3}$, respectively, while the layers thickness is set as 0.004 μm , 0.01 μm , 0.4 μm and 0.5 μm , respectively. The simulated parameters for the basic solar cell are J_{sc} of 40.03 mA/cm^2 , V_{oc} of 0.94 V, P_{max} of 30.8 mW/cm^2 , fill factor of 82.19% and efficiency of 22.9%. A balanced variation for the doping concentration and thickness for all layers of the basic solar cell have been investigated. Out of variation the doping concentration and thickness simulation it is concluded that:

The acceptor doping concentration for window layer has weak impact on the value of all cell parameters, besides, the thickness of window should be as low as possible to ensure the maximum amount of photon transmitted into the active region.

Increasing the doping concentration for emitter does not much effect on cell parameters, while increasing the thickness has more obviously impact and slightly increases the cell efficiency.

Higher doping concentration for base degrades the performance of the cell significantly due to the high recombination rate, while increasing the thickness remarkably improves the cell performance due to the increase of absorption probability for the photons of longer wavelength.

The doner doping concentration and thickness for BSF layer remarkably increases all cell parameters due to its ability to repel the photogenerated carriers and confine them within the active region.

The optimized solar cell is achieved at doping level of $3 \times 10^{18} \text{ cm}^{-3}$, $1 \times 10^{18} \text{ cm}^{-3}$, $3 \times 10^{17} \text{ cm}^{-3}$ and $1 \times 10^{22} \text{ cm}^{-3}$, respectively, and thickness of 0.005 μm , 0.36 μm , 1.7 μm and 2 μm , respectively. Whereas the simulated parameters for optimized cell are J_{sc} of 52.58 mA/cm^2 , V_{oc} of 1 V, P_{max} of 46.86 mW/cm^2 , fill factor of 88.54% and efficiency of 33.94%.

Using AlGaInP as BSF layer with the bandgap of 2.4 eV gives better cell performance as compared to AlGaAs that is used mostly in literature, besides, it shows high photogeneration rate indicating that it has rule of increasing the efficiency of the proposed cell.

Generally, the results confirm that engineering the doping concentration and thickness for solar cell layers has significant impact on improving the cell performance.

References

- [1] K. C. Devendra, R. Wagle, R. Gaib, A. Shrivastava, L. Nath Mishra, American Journal of Engineering Research (AJER) 9(4), 218 (2020).
- [2] E. T. Mohamed, A. O. M. Maka, M. Mehmood, A. M. Direedar, N. Amin, Sustainable Energy Technologies and Assessments 44, 101067 (2021); <https://doi.org/10.1016/j.seta.2021.101067>
- [3] C. Palacios, N. Guerra, M. Guevara y M. López, Revista de I+D Tecnológico 14(2), 96 (2018); <https://doi.org/10.33412/idt.v14.2.2078>
- [4] P. P. Nayak, J. P. Dutta, G. P. Mishra, Engineering Science and Technology, an International Journal 18, 325 (2015); <https://doi.org/10.1016/j.jestch.2015.01.004>
- [5] S. M. Lee, A. Kwong, D. Jung, J. Faucher, L. Shen, R. Biswas, M. L. Lee, J. Yoon, ACS Nano, 9(10), 10356 (2015); <https://doi.org/10.1021/acsnano.5b05585>
- [6] A. Hemmani, B. Dennai, A. Nouri, H. Khachab, B. Dekkich, Journal of Ovonic Research 13(6), 307 (2017).
- [7] K. Attari, L. Amhaimar, A. Elyaakoubi, A. Asselman, M. Bassou, International Journal of Photoenergy 2017, 8269358 (2017); <https://doi.org/10.1155/2017/8269358>
- [8] D. J. H. Victor, M. D. Jackuline, D. Gracia, Przegląd Elektrotechniczny 12, 9 (2020).
- [9] C. F. Kamdem, A. T. Ngoupo, F. K. Konan, H. J. T. Nkuissi, B. Hartiti and J. Ndjaka, Indian Journal of Science and Technology 12(37), 1 (2019); <https://doi.org/10.17485/ijst/2019/v12i37/147207>

- [10] A. Imran, M. Sulaman, Y. Song, D. Eric, M. N. Zahid, M. Yousaf, M. I. Saleem, M. Li, D. Li, *Journal of Computational Electronics* 20, 310 (2021); <https://doi.org/10.1007/s10825-020-01583-6>
- [11] M. Azza, E. Chahid, A. Hmairrou, R. Abdia, M. Tridane, A. Malaoui, S. Belaaouad, *Biointerface Research in Applied Chemistry* 13 (4), 253 (2023).
- [12] M. Abderrezek, F. Djahli, M. Fathi, M. Ayad, *Elektronika Ir Elektrotechnika*, 19(8), 41 (2013); <https://doi.org/10.5755/j01.eee.19.8.5392>
- [13] A. Talhi, A. Belghachi, H. Moughli, B. Amiri, L. Varani, *Digest Journal of Nanomaterials and Biostructures* 11(4), 1361 (2016).
- [14] F. Djaafar, B. Hadri, G. Bachir, *International Conference on Recent Advances in Electrical Systems, Tunisia*, (2017).
- [15] M. S. Salem, O. M. Saif, A. Shaker, M. Abouelatta, A. J. Alzahrani, A. Alanazi, M. K. Elsaid, R. A. Ramadan, *International Journal of Photoenergy* 2021, 8842975 (2021); <https://doi.org/10.1155/2021/8842975>
- [16] Y. Zhao, C. Liang, M. Sun, Q. Liu, F. Zhang, D. Li, Z. He, *Journal of Applied Physics* 116, 154506 (2014); <https://doi.org/10.1063/1.4898692>
- [17] J. Hossain, *Journal of Physics Communications*, 5(8), 085008 (2021); <https://doi.org/10.1088/2399-6528/ac1bc0>
- [18] F. Azzemou, D. Rached, W. L. Rahal, *Optik* 217, 164802 (2020); <https://doi.org/10.1016/j.ijleo.2020.164802>
- [19] S. M. Shamim, A. Sarker, M. R. Ahmed, F. Huq, *International Journal of Computer Applications*. 113(14), 8 (2015); <https://doi.org/10.5120/19893-1904>
- [20] M. Ramamurthy, D. Abishek, B. Logesh, S. S. K. Prasad, *Indian Journal of Science and Technology*, 12(37), 1 2019; <https://doi.org/10.17485/ijst/2019/v12i9/141996>